Decision-making methodology for managing photovoltaic surplus electricity through Power to Gas: combined heat and power in urban buildings

Manuel Bailera[a*], Begoña Peña[a], Pilar Lisbona[b], Luis M Romeo[a]

[a] Escuela de Ingeniería y Arquitectura. Universidad de Zaragoza, Campus Río Ebro, María de Luna 3, 50018, Zaragoza, Spain
[b] Escuela de Ingeniería de la Industria Forestal, Agronómica y Bioenergía. Universidad de Valladolid, Campus Duques de Soria, 42004, Soria, Spain

Abstract

Power to Gas technology, which converts surplus electricity into synthetic methane, is a promising alternative to overcome the fluctuating behavior of renewable energies. Hybridization with oxy-fuel combustion provides the CO_2 flow required in the methanation process and allows supplying both heat and electricity, keeping the CO_2 in a closed loop. The complexity of these facilities makes their management a key factor to be economically viable. This work presents a decision-making methodology to size and manage a cogeneration system that combines solar photovoltaic, chemical storage through Power to Gas, and an oxy-fuel boiler. Up to 35 potential situations have been identified, depending on the surplus electricity, occupancy of the intermediate storages of hydrogen and synthetic methane, and thermal demand. For illustration purposes, the methodology has been applied to a case study in the building sector. Specifically, a building with 270 kW of solar photovoltaic installed power is analyzed under nine energy scenarios. The calculated capacities of electrolysis vary from 65 kW to 96 kW with operating hours between 2184 and 2475 hours. The percentage of methane stored in the gas grid varies from 0.0% (no injection) to 30.9%. The more favorable scenarios are those with the lowest demands, showing temporary displacements beyond the month between injection and utilization.

Keywords

Power-to-Gas, Oxy-fuel combustion, Methanation, Renewable energy, Energy storage, Cogeneration

Corresponding author: mbailera@unizar.es

1. Introduction

One of the targets of the European Union for 2020 is the achievement of a 20% of renewable energy in the overall energy mix with a 20% reduction in CO_2 emissions [1]. It is clear that renewables will continue playing a key role in helping the EU reducing pollutant emissions, increasing energy security (using renewable and autonomous energy and diversifying energy sources) and meeting its energy needs beyond 2020. According to the trends to 2050 from the "EU Reference Scenario 2016", the share of electricity produced from renewables is expected to grow up to 37.2% by 2020, 43% by 2030, and 53% by 2050 [2].

The main barriers associated to renewable energy sources (RES) are related to the management of fluctuations due to the intermittent nature of this kind of power generation. Mainly, the mismatches between supply and electrical demand affect security and stability of the grid and represent an important barrier for the technical and economic feasibility of RES and, in consequence, for their final expansion.

The achievement of the ambitious objectives for RES and the deployment of a diversified energy system, where the energy production fits the instantaneous demand, require the proposal and development of innovative energy storage solutions. Current technologies (pumped hydroelectric storage, compressed air energy storage, flywheels and batteries) present a low energy density and/or narrow growth potential (hundreds of MWh) [3]. These limitations could make Power to Gas (PtG) technology one promising option to overcome these restrictions and increase reserve production ratios. Moreover, it would be very desirable for these new concepts to supply not only electricity but also heat to the final users. In these situations, the usual alternatives for energy storage do not represent a feasible solution. For cogeneration applications, PtG technology represents the only suitable option. Power stations [4], industries [5] and tertiary sector applications, as buildings [6] or transport [7], are representative examples for applying PtG concept to hybrid polygeneration systems.

Under a scenario with massive renewable generation, PtG processes appear as promising alternatives to convert electricity into synthetic natural gas (SNG, renewable methane). The features of this technology allow to chemically store, in the form of CH_4, the surplus electricity of a non-regulated generation system, while reusing CO_2 from a source of pollutant emissions. Different PtG concepts, such as hybridization with air

separation plants, biogas plants, biomass gasification, sewage plants, fossil power plants or industrial processes, have been proposed to integrate the source of carbon dioxide [8]. In all cases, the utilization of the residual oxygen produced by electrolysis [9] and the energy consumption to attain a concentrated stream of CO_2 are the key points to reach a competitive technology.

The coupling of hydrogen production by electrolysis fed with RES and the Sabatier reaction (Eq. 1) is one of the possibilities to produce synthetic methane. The reaction of hydrogen and carbon dioxide produces methane through two consecutive reactions: inverse water-gas shift reaction (Eq. 2) and CO methanation (Eq. 3) [10].

$$CO_2 + 4H_2 \leftrightarrow CH_4 + 2H_2O \qquad \Delta H_{298K} = -164.9\ \text{kJ/mol} \qquad (1)$$

$$CO_2 + H_2 \leftrightarrow CO + H_2O \qquad \Delta H_{298K} = +41.5\ \text{kJ/mol} \qquad (2)$$

$$CO + 3H_2 \leftrightarrow CH_4 + H_2O \qquad \Delta H_{298K} = -206.4\ \text{kJ/mol} \qquad (3)$$

Eq. 2 is an endothermic reaction that requires the presence of a catalyst to take place at low temperature, and promotes conversion to methane in Eq. 3.

Through this process, besides to store electricity surplus, the obtained SNG is nearly neutral in CO_2 emissions if RES are used. Although it has been demonstrated that CO_2 capture and utilization (CCU) is not by itself a useful technology to remarkably mitigate climate change [11], the hybridization of PtG with oxy-combustion [6,9] really avoids additional emissions in the use of natural gas by using CO_2 recycling and RES. This means an actual reduction in CO_2 emissions with respect to conventional combustion facilities.

The surplus electricity storage in the form of methane implies the connection of electric and gas networks in a single energy system introducing high flexibility in the grid balance, with the advantage of not requiring additional infrastructures. He et al. showed that wind power curtailment can be reduced a 97% thanks to Power to Gas under some scenarios [12], Li et al. found that Power to Gas is effective on improving the wind power utilization rate and contributes on the reduction of natural gas consumption [13], while McKenna et al. stated that Power to Methane is expected to be an option in the next decades on a local level due to the restrictions for injecting hydrogen into the gas network [14]. However, the smart management of the intermittent and fluctuating surplus, the variable consumption of power and heat and the storage of

intermediate and final species is a very complex challenge to reach an integrated network that guarantees the stability of supply with a positive economic balance.

Smart regulation and scheduling are also crucial and complex for polygeneration systems based in the proposed combination of heat, power and SNG production (and/or even other chemicals), as all the processes are usually simultaneous and fluctuating according to the respective demand [15]. A thorough analysis must be done, as the number of operating hours could be insufficient and the feasibility studies risky. In this scenario, control strategies to manage the excess generation from RES will play an essential role in the feasibility studies of these systems.

Recent studies have presented a simplified methodology for determining the price ratio of the electrical energy sales to the purchase price of electricity to make economically attractive the hydrogen production technology applied to PtG [16]. A power management methodology based on multi-objective optimization techniques has been used in an autonomous hybrid system of RES, energy storages and energy generators in order to optimize the tilt angles of photovoltaic panels and the tower height for wind turbines [17]. Moreover, there are also some probabilistic optimal power flow models to simulate the operation of coupled electric power and natural gas systems multiple periods to avoid overly-optimistic solutions in the design [18]. Similar works [19] also consider the natural gas, heat, and power demand balances when are applied to wind power and a PtG unit. Finally, both techno-economic and life cycle assessment (LCA) were applied to determine key performance indicators for PtG system both from a stationary operation [20] and a dynamic point of view [21]. In these cases, the objective was to determine the performance, levelized cost and value of PtG plants purchasing electricity and selling gas market, depending on the system configuration under a specific regulatory context.

This work aims to lay the fundamentals of an eventual control system for a hybrid system combining RES with energy storage through PtG. A novel methodology to identify restrictions and the potential situations to be managed in this kind of facilities is developed and applied to a realistic case study of the building sector for illustration purposes. The novelty relies in the application of Power to Gas as long-term energy storage for zero-emission buildings. Depending on the RES availability and the thermal and power demands, different

scenarios are found with excess or deficit of power and thermal energy. Therefore, the final user has to choose the best strategy for every situation, which changes throughout seasons, months and days.

The presented methodology is useful for designing, sizing and efficiently operating those energy storage installations based on PtG that are integrated in the natural gas network. It will serve as basis of advanced control algorithms to reach a positive economic balance. Although there are some recent works that deal with this economic issue for PtG (Guilera et al. compared the levelized cost of SNG with the market price of conventional natural gas [22], while Götz et al. gathered some other economic studies in their review article [23]), it is a topic that has not been yet explored in the literature with the detail and the practical point of view of the present study. The analysis of the concept provides the framework of application of this kind of systems, and the technical limitations in terms of size of equipment, solar irradiation, and electric and thermal demands to satisfy. Results are crucial for further studies to properly perform economic optimizations. The equipment sizing and the decision-making methodology can be completely used in this (and others) type(s) of installations that are compelled to adapt renewable electricity production to the demand patterns of urban buildings.

After this introduction, the proposed integrated system is described (Section 2), the notation used in the following sections is introduced and the model developed in Aspen Plus® is explained (Section 2.1). Then, the specific case study is presented (sports centers), together with the nine analyzed scenarios of generation and demand (Section 3). Methodology section presents the sizing of the system according to solar irradiation and energy demands (Section 4.1 and Section 4.2), and the mathematical description of every operating situation that may take place during the year and the decision tree (Section 4.3). Finally, the results section discusses the surplus electricity management (Section 5.1), the case distribution of the decision tree (Section 5.2) and the temporary displacement of the stored energy (Section 5.3).

2. Solar photovoltaic, Power to Gas and Oxy-fuel boiler integrated system

According to the energy framework outlined by the EU for the near future, hybrid polygeneration systems using RES and energy storage will be developed to supply heat and power. The most interesting application is

the building sector where both, heat and power, are demanded in similar proportion and CO_2 emissions are very difficult to be controlled.

Since photovoltaic (PV) technology is the most suitable among RES to be adapted to this sector, the hybrid system proposed in this study to cover the different energy demands couples PV panels, PtG and an oxy-fuel boiler. The hybridization of PtG with oxy-fuel boiler produces a double positive synergy as it is presented in Fig. 1: oxy-fuel boiler acts as a source of concentrated CO_2 for methanation process and it takes advantage from the O_2 by-produced during the electrolysis stage. This oxygen serves as direct comburent in the boiler avoiding the use of an air separation unit to obtain the oxygen. The different energy fluxes (W-electrical, P-chemical, Q-thermal), as well as the performance towards chemical energy (η) and the efficiency towards thermal energy (ε) of each equipment are indicated in Fig. 1 with the nomenclature used in the following sections.

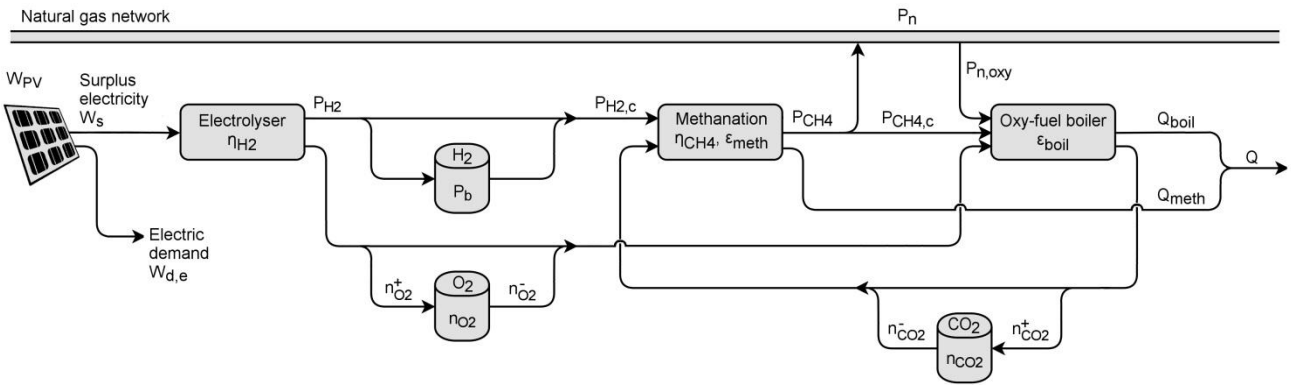

Figure 1. *PtG-Oxyfuel boiler integration scheme*

A wide variety of energy demand scenarios may be assessed, and the PV-PtG-Oxyfuel system might represent only a part of the thermal supply in some of them. Therefore, it will be assumed that, in general, the building maintains conventional air-fired boilers to support the thermal demand. Nevertheless, the required ASU for a hypothetical oxy-fuel boiler to cover the whole demand will be sized, as oxygen from the electrolysis would be insufficient in that case. The ideal case would be the avoidance of the complementary air-fired boiler and the ASU.

Excess power from PV panels (W_s) will be chemically stored through the PtG subsystem in the form of methane. In the general case, the oxy-fuel boiler together with the exothermal heat from methanation stage will partly cover the thermal demand of the analyzed facility ($Q_{boil} + Q_{meth}$). Whenever the methane production exceeds thermal demand in the oxy-fuel boiler, methane will be injected into the gas grid to be consumed in other periods with insufficient production. In such cases, after being recovered from the grid, natural gas will be consumed in the oxy-fuel boiler whenever possible ($P_{n,oxy}$); otherwise, methane will feed the air-fired boiler (not shown in Fig. 1).

Additionally, buffers of H_2, O_2 and CO_2 are required to manage surplus and deficiencies of these species. Surplus of hydrogen will exist when production exceeds the amount that can be treated by the methanation plant and it will lack when its production is not enough to convert the CO_2 coming from the oxy-fuel boiler. Regarding oxygen, there will be an excess (n_{O2}^{+}) when not all the produced methane is consumed (under low thermal demand) and it will lack (n_{O2}^{-}) when additional natural gas has to be recovered from the network to cover the thermal demand. According to the stoichiometry, there will be a surplus of carbon dioxide (n_{CO2}^{+}) when the methane is consumed faster than produced, and there will be a shortage of carbon dioxide (n_{CO2}^{-}) when methanation is not operated at full load although there is enough hydrogen production.

2.1 Power to Gas-Oxyfuel boiler model

The PtG-oxyfuel boiler subsystem has been modeled in Aspen Plus® in order to evaluate the performance under realistic conditions. The developed simulation uses the 'PSRK property method' provided by Aspen Plus®. This package is based on the predictive Soave-Redlich-Kwong equation-of-state model, whose parameters are calculated through the Holderbaum-Gmehling mixing rules. The interaction parameters to be introduced in the mixing rules are directly provided by the Aspen Plus® database. Besides, it is assumed chemical equilibrium and steady state operation in every simulated process (methanation, oxy-fuel combustion, etc.). As a first approach, the conditions of production and consumption are analyzed in hourly periods, considering that the solar irradiation and the heat and electricity demands are constant for every hour.

The combustion of natural gas uses an RGibbs unit, which calculates the equilibrium of the reaction by minimizing the Gibbs free energy. The sensible heat of the combustion gas (Q_{boil}) is transferred to produce

hot water. After this, a flue gas temperature of 270 ºC is achieved, which is used to preheat the recycled flue gas up to 180 ºC (hence, the final temperature of flue gas is 190 ºC). The exhaust gas stream is partially recycled into the boiler (79%), and partially fed to the methanation system (21%). The comburent in the oxy-fuel boiler is composed by O_2 from electrolyzer, plus partially-dried flue gas.

Electrolyzer model is based on a user-modeled unit that splits water in pure oxygen and a mixture of hydrogen and water. The conversion of water in this device reaches 99.9%, and the electrical consumption is set at an optimistic value for alkaline electrolyzers of 4.2 kWh/Nm^3H_2 [23], thus taking into account the fact that electrolyzer will work mostly below the nominal load and that the efficiency increases at partial loads [24]. These operating conditions lead to a thermal efficiency of $\eta_{H2} = 70\%$ (LHV basis). Methanation stage is composed of two isothermal reactors at 10 bar and 350 ºC modeled through two RGibbs units, with an intermediate water condenser. The final synthetic natural gas achieves a 95% volume fraction of methane. The conversion efficiency of the methanation stage is $\eta_{CH4} = 81.1\%$ (energy content ratio between produced SNG and H_2 input), and the thermal efficiency of the boiler is $\varepsilon_{boil} = 85\%$. Moreover, the exothermal heat from methanation reaction (Q_{meth}) is quantified as a useful output of the system, being integrated to produce domestic hot water. A 20% loss of the available heat is assumed: $\varepsilon_{meth} = (1 - \eta_{CH4}) \cdot 0.8$. Effect of partial load operation on performance of methanation and oxy-fuel boiler is not significant.

3. Case study and proposed scenarios

The integration of photovoltaics and Power to Gas in urban buildings with large roof areas allows providing electricity at the same time that surpluses are converted into methane. Thus, facilities with moderate heating demands that use natural gas boilers are potential users of this renewable cogeneration system (e.g., heated indoor pools, shopping malls, resorts).

In the present study, the application of PtG-Oxyfuel system coupled to PV panels is assessed to cover the demand of sports centers in Zaragoza (Spain). The order of magnitude of the roof for this kind of buildings has been quantified by means of the Google Maps tool, ranging from 1300 to 3600 m^2. A medium building with 2600 m^2 of roof surface is considered for the case study, but in practice only the 70% of the roof area is

available for installing PV panels (i.e., 1820 m^2). Thus, the nominal power (Eq. 4) of the PV system that could be installed is 273 kW, given by:

$$W_{PV,0} = \mathrm{A}_{\mathrm{roof}} \cdot I_0 \cdot \eta_{\mathrm{PV},0} \tag{4}$$

where $I_0 = 1\ kW/m^2$ is the maximum solar irradiance on a clear day, and a nominal efficiency $\eta_{\mathrm{PV},0} = 15\%$ has been considered [25]. The actual solar irradiance through the year is obtained from PVGIS Tool (Photovoltaic Geographical Information System) [25] to calculate the profile of PV production, in which it is only considered an average day for every month (the average day of July will be shown in Fig. 7). According to that, the annual renewable production for the selected location and PV area is 433.8 MWh.

The most important electrical demands for the buildings under study come from dehumidifiers, lighting, and pumps, followed by air conditioners, appliances and computers. The typical total electric demand, $E_{d,e,}$ may span in the range 300 – 700 MWh/y depending on the size of the center (Píriz A. studied the electric consumption in a heated swimming pool [26], and Ducar I. in a Sports centre [27], both placed in Zaragoza). Therefore, three scenarios of electric consumption are proposed, based on the ratio between de electric energy demand and the generated electricity through PV, $E_{d,e}/E_{PV} = [1.25, 1.00, 0.75]$.

The monthly load profile for electricity demand has been taken from a real energy audit (Fig. 2) [27] and then properly scaled to the analyzed electric demand scenarios. The pattern shows a peak of consumption in June and July due to the cooling necessities, a stable period between October and March, and a drop for April and May. The hourly demand is simplified by considering 100% load when the center is open, and 55% when it is closed, as dehumidifiers keep working.

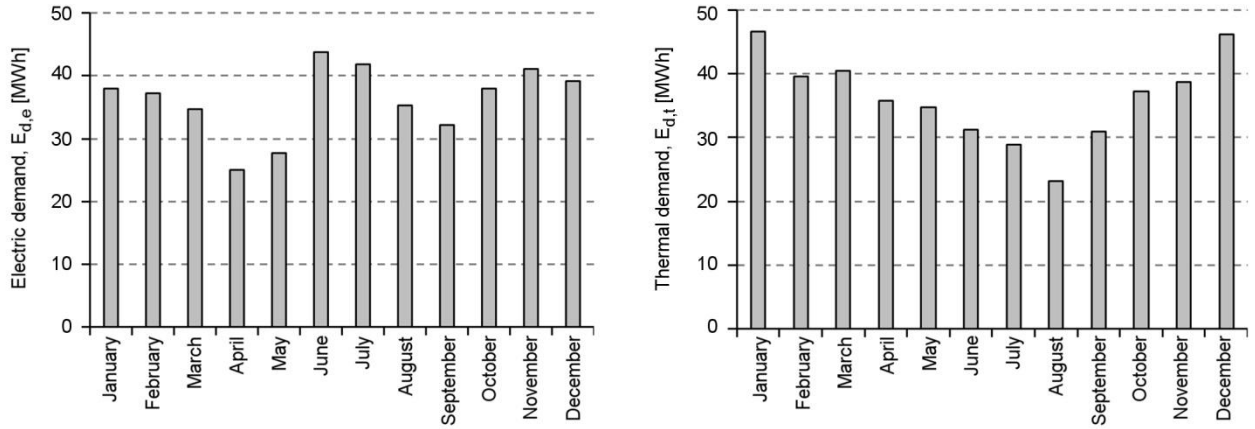

Figure 2. Monthly electric and thermal energy demand for $E_{d,e}/E_{PV} = 1.00$ and $E_{d,t}/E_{d,e} = 1.00$.

Annual thermal demands ($E_{d,t}$) in sports centers are mainly for indoor pools heating purposes, as well as for producing domestic hot water and heating the building. Typical consumptions widely vary from 200 to 1000 MWh/y depending on the location and the services of facilities. Three scenarios are considered according to the ratio between the thermal energy demand and the electric energy demand: $E_{d,t}/E_{d,e} = [1.00, 0.75, 0.50]$. Monthly demand along the year follows the profile shown in Fig. 2, according to the real data of an energy audit [27], properly scaled to the proposed thermal scenarios. The load curve clearly shows a seasonal behavior where consumption increases during the coolest months. The hourly demand is simplified by considering 100% load when the center is open, and 70% when it is closed, as pool heating keeps working.

In summary, by combining the potential demands of electricity and thermal energy, a total of 9 scenarios arise. The specified values for $E_{d,t}/E_{d,e}$ and $E_{d,e}/E_{PV}$ ratios aim to cover different locations (solar irradiance), weathers (thermal consumption), and sport centers' equipment (electric consumptions). The main global magnitudes are gathered in Table 1.

Table 1. Scenarios under study, considering the demand profiles of Fig 2.

Scenario	**1**	**2**	**3**	**4**	**5**	**6**	**7**	**8**	**9**
Ratio $E_{d,e}/E_{PV}$	1.25	1.25	1.25	1.00	1.00	1.00	0.75	0.75	0.75
Ratio $E_{d,t}/E_{d,e}$	1.00	0.75	0.50	1.00	0.75	0.50	1.00	0.75	0.50
Electric demand ($E_{d,e}$) [MWh/y]	542.3	542.3	542.3	433.8	433.8	433.8	325.3	325.3	325.3
$E_{d,e}$ covered by E_{PV} [%]	46.7	46.7	46.7	48.6	48.6	48.6	50.0	50.0	50.0
Surplus electricity from E_{PV} [MWh/y]	179.1	179.1	179.1	222.9	222.9	222.9	270.9	270.9	270.9
Thermal demand ($E_{d,t}$) [MWh/y]	542.3	406.7	271.1	433.8	325.3	216.9	325.3	244.0	162.7

4. Methodology

The different parts of the integrated system are here sized according to the available PV production, electricity demand and thermal requirements. Then, the operation is evaluated through a decision-making strategy based in 35 potential situations of surplus electricity related to the hydrogen production, the thermal demand and the occupancy of the buffers of hydrogen, oxygen and carbon dioxide.

The electrolyzer is sized in order to maximize the amount of electricity that is yearly stored at nominal load, according to the historical data series. The followed methodology is based on the so-called Load Duration Curve (Subsection 4.1).

The oxy-fuel boiler that is coupled with the PtG system is design afterwards in Subsection 4.2. The urban building is assumed to have an already existing facility that satisfies its thermal requirements with a conventional air-fired boiler fed with natural gas. The study assesses the commissioning of a PtG facility, which stores the surplus electricity, and a small oxy-fuel boiler that complements the air-fired boiler. This oxy-fuel boiler will consume the SNG when available in order to decarbonize a part of the thermal supply that was satisfied by the air-fired boiler until now. Then, as the scenarios progress from 1 to 9 (see Table 1), the available surplus electricity increases, and the thermal production of the oxy-fuel boiler becomes more important. At some point, the oxy-fuel boiler will be large enough to completely replace and decommission the air-fired boiler that the urban building originally had. It should be noted that, in those situations in which the air-fired boiler has been decommissioned, if natural gas is purchased due to the temporary lack of SNG, it will be consumed in the oxy-fuel boiler. As oxygen is produced in stoichiometric amount with respect to the SNG by the electrolyzer, to fired additional methane implies the necessity of implementing an auxiliary ASU for the shortages of SNG.

Once the design is fixed, the hourly operation of the facility is finally analyzed (Subsection 4.3). The presented methodology characterizes every potential situation that could take place throughout the year. This analysis considers different energy flows (power units). The energy storage rate, in terms of hydrogen produced by the electrolyzer, is denoted by P_{H2}, while the thermal energy production rate that can be achieved with that flow of hydrogen is denoted by Q_{H2}. The latter includes the exothermal heat from methanation and the thermal energy released in the boiler. In addition, P_b represents the maximum consumption rate of the stored hydrogen considering that the buffer is depleted in 1 hour, while Q_b is the thermal energy production rate associated to its consumption. Moreover, the rate at which heat can be produced by consuming in an hour the SNG previously stored in the network, Q_n, must be also included to finally compare the whole available thermal energy with the actual thermal demand, Q_d.

A decision tree is built to quantify the amount of H_2 and SNG that must be consumed to cover the energy demand, as well as the natural gas that must be purchased if required. It also identifies whether the H_2 buffer and the gas network are gathering the excess or supplying the stored gases (the capacity of the buffers will be considered unlimited, hence the maximum occupancy achieved during the year will determine the required size). However, the decision tree does not distinguish whether the recovered SNG should be fed into the oxy-fuel boiler or into the air-fired boiler. It also does not deal with the O_2 and CO_2 management, for which additional equations will be provided in Table 2.

It should be noted that the usual notation for electric power, $\dot{W}$, and for thermal power, $\dot{Q}$, is simplified in this study as W and Q to avoid tedious notation due to the high number of equations. Hence E denotes energy variables to avoid misunderstandings (see Nomenclature section).

4.1. Electrolyzer sizing

The electrolysis installed capacity is sized in order to maximize the amount of electricity that is stored at nominal load. This has been quantified by using the Load Duration Curve, $W_{elec}(h)$, which depends on electricity demand and PV production profiles. Fig. 3 plots the electrolysis power versus the nominal operating hours that such installed capacity would have. The maximization of the area $E(h) = W_{elec}(h) \cdot h$ gives the optimal capacity $W_{elec,0} = W_{elec}(h_0)$, where h_0 represents the operating hours at nominal load for such electrolyzer capacity, satisfying the condition given in the Eq. 5:

$$E(h_0) = \max \{ E(h) \mid \mathrm{h} \in \mathbb{R}, \mathrm{h} > 0 \} \tag{5}$$

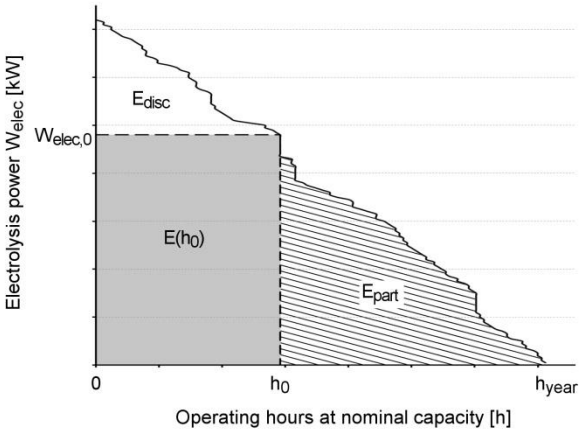

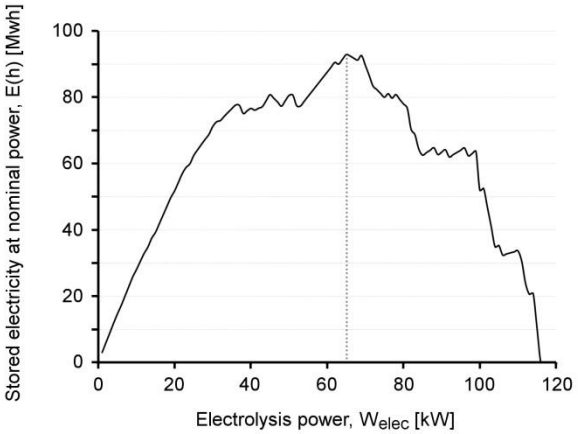

Figure 3. Left: Load duration curve: the shaded areas represent the stored energy at full or partial load. Right: Stored electricity at nominal power, $E(h)$ vs. Electrolysis power W_{elec} for $E_{d,e}/E_{PV} = 1.25$.

Thus, the equivalent operating hours of the electrolysis system, h_{elec}, including the partial load operation, is given by Eq. 6:

$$h_{elec} = h_0 + \frac{1}{W_{elec,0}} \int_{h_0}^{h_{year}} W_{elec}(h)dh = h_0 + \frac{E_{part}}{W_{elec,0}} \quad (6)$$

where $\boldsymbol{E_{part}}$ is the surplus electricity stored by the electrolyzer at partial load (see Fig. 3; $\boldsymbol{E_{disc}}$ is the discarded surplus electricity). The maximum rate of conversion to hydrogen carrier, if $\boldsymbol{\eta_{H_2}}$ is the efficiency of electrolyzer, is $\boldsymbol{P_{H_2,max} = W_{elec,0} \cdot \eta_{H_2}}$ and the actual H_2 production rate will be given by the current surplus of electricity, $\boldsymbol{W_s}$, by $\boldsymbol{P_{H_2} = W_s \cdot \eta_{H_2}}$.

4.2. Methanation and oxy-fuel boiler sizing

The maximum production of heat for a given electrolyzer capacity (Q_{max}) is composed of the thermal energy from the oxy-fuel boiler and the integrated exothermal heat from methanation stage (Fig. 1), according to Eq. 7:

$$Q_{max} = Q_{meth} + Q_{boil} = W_{elec,0} \cdot \eta_{H_2} \cdot (\varepsilon_{meth} + \eta_{CH4} \cdot \varepsilon_{boil}) \quad (7)$$

However, there will be scenarios in which the maximum hourly demand, $Q_{d,max} = \max(Q_d)$, is much lower than Q_{max}, and therefore the corresponding stages of methanation and oxy-fuel boiler would be oversized. In order to analyze those situations, we define the producible heat of the PtG-Oxyfuel boiler system, Q_{100}, as a function of the nominal input of the methanation plant, $P_{meth,0}$:

$$Q_{100} = P_{meth,0} \cdot (\varepsilon_{meth} + \eta_{CH4} \cdot \varepsilon_{boil}) \quad (8)$$

If Q_{max} is lower than the maximum thermal demand, there is no limitation and the methanation nominal input, $P_{meth,0}$, will be sized equal to the nominal H_2 production (see Eq. 9). Besides, the nominal input of the oxy-fuel boiler, $P_{boil,0}$, will be the nominal production of SNG (i.e., the size of a subsystem is set by the preceding one). These conditions are summarized as follows:

$$\text{if } Q_{max}\begin{cases} < Q_{d,max}, & \text{then } P_{meth,0} = W_{elec,0}\cdot\eta_{H_2}, \quad P_{boil,0} = P_{meth,0}\cdot\eta_{CH_4} \\ > Q_{d,max}, & \text{then } P_{meth,0} = \frac{Q_{d,max}}{(\varepsilon_{meth}+\eta_{CH4}\cdot\varepsilon_{boil})}, \quad P_{boil,0} = P_{meth,0}\cdot\eta_{CH_4}\left(1+\frac{\varepsilon_{meth}}{\eta_{CH4}\cdot\varepsilon_{boil}}\right) \end{cases} \quad (9)$$

Conversely, if the nominal hydrogen production allows providing more thermal energy than the maximum thermal demand, the methanation nominal input has to be scaled down to match the producible heat and the maximum demand: $Q_{100} = Q_{d,max}$. Otherwise, the methanation system would be oversized. In this case, the air-fired boiler loses its relevance and the oxy-fuel boiler should be sized to fulfil maximum demand even when heat from methanation is not available, i.e., when SNG is recovered from the gas network.

4.3. Operation analysis

The operation and management of the PV-PtG-Oxyfuel system at every hour will depend on the production of hydrogen ($P_{H2} = W_s \cdot \eta_{H_2}$), on the thermal energy that is demanded (Q_d), on the amount of hydrogen stored in the buffer and on the SNG available in the gas network. For the latter two variables, two consumption rates are defined (P_b and P_n) to consider the maximum energy power that can be extracted from the hydrogen buffer (P_b, emptying of the H_2 buffer in 1 hour) and from the natural gas network (P_n, depletion of the stored SNG in 1 hour). Additionally, the released heat corresponding to these input fuels are calculated, respectively, as: $Q_{H2} = P_{H2}\cdot(\varepsilon_{meth} + \eta_{CH4}\cdot\varepsilon_{boil})$, $Q_b = P_b\cdot(\varepsilon_{meth} + \eta_{CH4}\cdot\varepsilon_{boil})$ and $Q_n = P_n\cdot\varepsilon_{boil}$.

The decision-making algorithm (Fig. 4) firstly compares the hydrogen production, P_{H2}, with the maximum ($P_{100} \equiv P_{meth,0}$) and minimum ($P_{40} \equiv 0.40\cdot P_{meth,0}$) operating loads of the methanation system, in order to identify situations of (i) surplus hydrogen (cases 1-5 of temporary storage in buffer when $P_{H_2} > P_{100}$), (ii) use of stored hydrogen or (iii) shutdowns (if $P_{H_2} < P_{40}$, cases 16-35). For intermediate values, the production rate of hydrogen in the electrolyzer is enough to operate the integrated thermal system at partial load.

Secondly, thermal demand is evaluated with respect to: (i) the producible heat at nominal load, Q_{100}, (ii) the producible heat at minimum load, $Q_{40} = 0.40\cdot Q_{100}$, and (iii) the producible heat corresponding to the actual hydrogen production, Q_{H2}. If $Q_{H_2} < Q_{40}$, the system uses hydrogen from the buffer whenever is possible, otherwise methanation stage must be turned off. The other extreme situation is the case $Q_d > Q_{100}$, which is also possible, as the methanation nominal input was selected as $Q_{100} = Q_{d,max}$ from historical data, and a different scenario could take place in the future. As this particular case would be avoided considering a safety

margin for sizing of methanation stage, it is not considered in the present analysis. For intermediate operating conditions ($Q_d < Q_{100}$ and $Q_{H2} > Q_{40}$), the system stores methane in the gas network ($Q_d < Q_{H2}$) or operates with support of H_2 buffer or stored SNG ($Q_{100} > Q_d \geq Q_{H2} > Q_{40}$).

When necessary, next step checks if the total hydrogen ($P_{H_2} + P_b$) is enough to operate the methanation system ($P_{H_2} + P_b > P_{40}$) or, on the contrary, methanation will be turned off and the hydrogen production will be stored while the thermal demand is covered by the gas network (just SNG or SNG plus purchased natural gas, depending on the case). If $\left(P_{H_2} + P_b\right) > P_{100}$, the extra energy is stored in hydrogen buffer and, if possible, as SNG in the network.

Finally, the current thermal energy generated with own fuels ($Q_{H_2} + Q_n + Q_b$) is compared with the thermal demand, to identify situations of self-consumption or cases in which the purchase of natural gas is necessary.

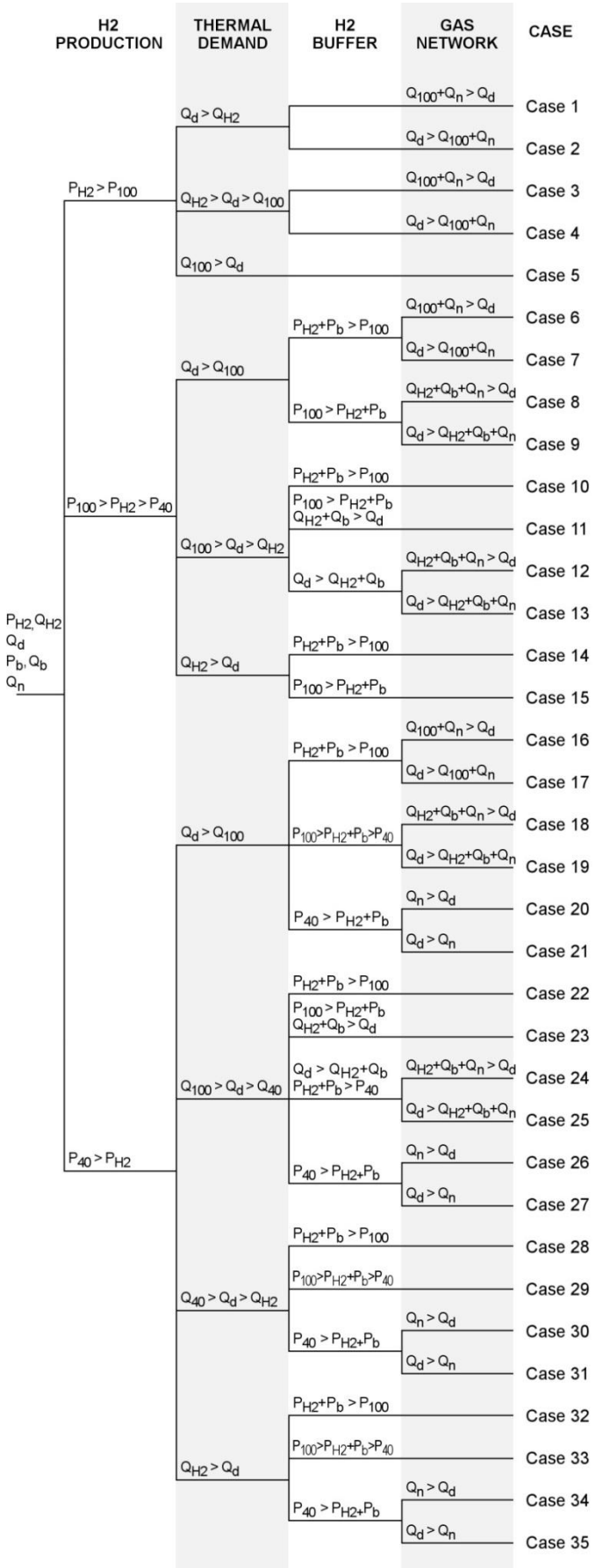

Figure 4. Decision tree for managing the PV-PtG-Oxyfuel system with H_2 buffer and SNG storage

A total of 35 potential cases have been found, which are depicted in Fig. 5 for better understanding. For example, in case 1 (Fig. 6), electrolysis produces more hydrogen than the maximum consumption capacity of the methanation stage ($P_{H2} > P_{100}$), while thermal demand is above the producible heat ($Q_d > Q_{100}$). It means that demand cannot be covered with the heat released in the integrated facility (Eq. 8). Nevertheless, the energy power that can be produced in the current hour by consuming all the SNG previously stored in the gas grid (P_n), allows satisfying the thermal demand ($(Q_{100} + Q_n) > Q_d$). It is also remarked the fact that $Q_d > Q_{H2}$ because it implies that oxygen is in deficit in order to introduce the recovered SNG from the network into the oxy-fuel boiler (see Appendix), contrarily to case 3.

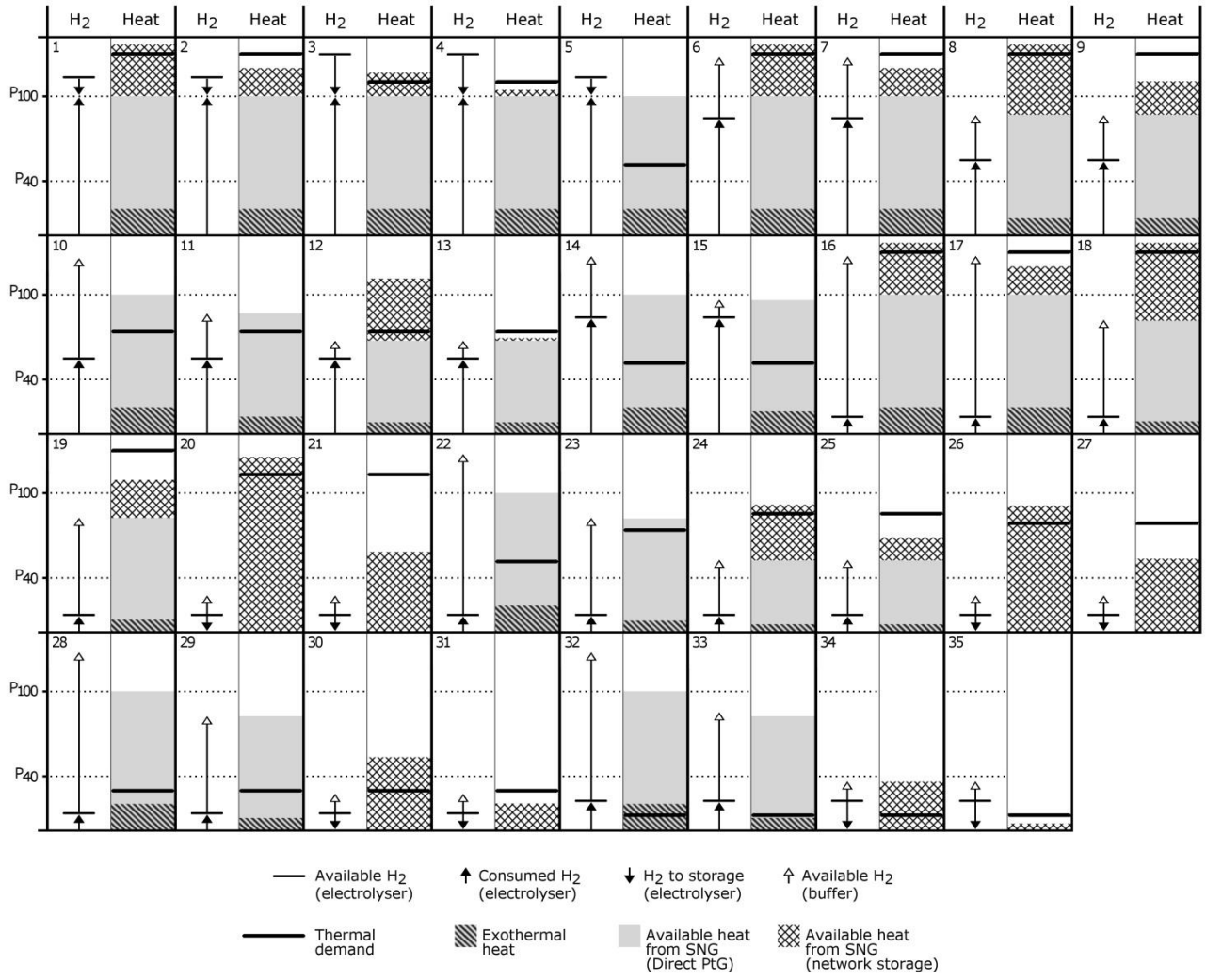

Figure 5. Graphical representation of the potential cases of the decision tree

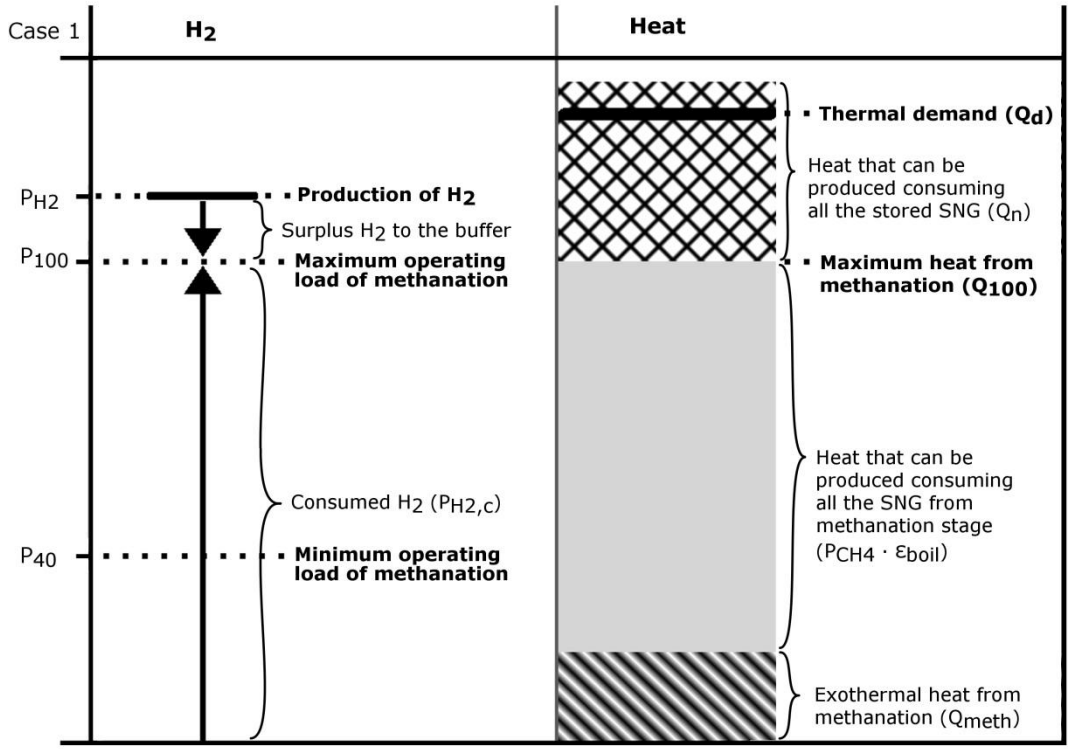

Figure 6. Graphical representation of Case 1 of the decision tree

In case 5, for example, there is surplus hydrogen that is sent to the buffer ($P_{H2} > P_{100}$) and surplus SNG that is stored in the gas network ($Q_{100} > Q_d$). In case 10, the produced hydrogen is not enough to satisfy thermal demand ($Q_d > Q_{H2}$), but the methanation can be operated at nominal load ($P_{H2} + P_b > P_{100}$) thanks to the stored hydrogen in the buffer and the extra SNG can even be stored in the gas network ($Q_{100} > Q_d$). Further details about the wide variety of situations may be examined in Fig. 5.

Most of the parameters that are calculated to describe the system can be defined with one single formula for all 35 cases (Table 2). The dependence on the variety of cases only needs to be considered in four of the variables from which they are computed (Table 3). These variables are the hydrogen consumption ($P_{H2,c}$), the renewable thermal energy production (Q, based on consumed SNG plus integration of exothermal heat), the amount of SNG that is produced in the PtG system and directly consumed ($P_{CH4,c}$), and the amount of SNG that is consumed from the gas network storage ($P_{n,c}$).

In order to avoid an excessively complex decision tree, special situations are considered during the calculation of some variables. When assessing the amount of SNG that is consumed, there may be a possibility that the

exothermic heat from methanation is enough to fulfil demand (e.g., case 32 in Fig. 5). For this reason, Table 3 shows an additional decision-making step for some values of $P_{CH4,c}$. Besides, some of the variables described with single formula also need an extra step to simplify the decision-making tree. It is the case of surplus and deficit calculations for O_2 and CO_2, as well as of the computation of the amount of SNG that is recovered from the network and is consumed in the oxy-fuel boiler. In the latter case, it is just checked if the capacity of the oxy-fuel boiler is enough to burn the SNG coming from the gas network.

Table 2. Computed variables to describe the PV-PtG-Oxyfuel system

Variable	Description	Value at hour j
Q_{meth} [kW]	Exothermal heat	$Q_{meth} = P_{H2,c} \cdot \varepsilon_{meth}$
P_b [kW]	Maximum rate recovery of available H_2 in buffer	$P_{b\,(j)} = P_{b\,(j-1)} + P_{H2\,(j-1)} - P_{H2,c\,(j-1)}$
P_n [kW]	Maximum rate recovery of available CH_4 in gas network	$P_{n\,(j)} = P_{n\,(j-1)} + P_{CH4\,(j-1)} - P_{CH4,c\,(j-1)} - P_{n,c\,(j-1)}$
P_{CH4} [kW]	CH_4 produced	$P_{CH4} = P_{H2,c} \cdot \eta_{CH4}$
$P_{CH4,p}$ [kW]	Purchased CH_4 to fulfil demand	$P_{CH4,p} = (Q_d - Q)/\varepsilon_{boil}$
$P_{n,oxy}$ [kW]	CH_4 from network to the oxy-fuel boiler	$P_{n,oxy} = \begin{cases} P_{boil,0} - P_{CH4,c} & \text{if } P_{CH4,c} + P_{n,c} > P_{boil,0} \\ P_{n,c} & \text{if } P_{CH4,c} + P_{n,c} \le P_{boil,0} \end{cases}$
$P_{n,air}$ [kW]	CH_4 from network to the air-fired boiler	$P_{n,air} = P_{n,c} - P_{n,oxy}$
n^+_{O2} [kmol/h]	Surplus O_2	$n^+_{O2} = \begin{cases} \left(P_{H2} - \frac{P_{CH4,c} + P_{n,oxy}}{\eta_{CH4}}\right)/134 & \text{if } P_{H2} > (P_{CH4,c} + P_{n,oxy})/\eta_{CH4} \\ 0 & \text{if } P_{H2} \le (P_{CH4,c} + P_{n,oxy})/\eta_{CH4} \end{cases}$
n^-_{O2} [kmol/h]	Deficit O_2	$n^-_{O2} = \begin{cases} 0 & \text{if } P_{H2} > (P_{CH4,c} + P_{n,oxy})/\eta_{CH4} \\ \left(\frac{P_{CH4,c} + P_{n,oxy}}{\eta_{CH4}} - P_{H2}\right)/134 & \text{if } P_{H2} \le (P_{CH4,c} + P_{n,oxy})/\eta_{CH4} \end{cases}$
n_{O2} [kmol/h]	Total O_2 in the buffer	$n_{O2\,(j)} = n_{O2\,(j-1)} + n^+_{O2\,(j-1)} - n^-_{O2\,(j-1)}$
n^+_{CO2} [kmol/h]	Surplus CO_2	$n^+_{CO2} = \begin{cases} 0 & \text{if } P_{CH4} > P_{CH4,c} + P_{n,oxy} \\ (P_{CH4,c} + P_{n,oxy} - P_{CH4})/213 & \text{if } P_{CH4} \le P_{CH4,c} + P_{n,oxy} \end{cases}$
n^-_{CO2} [kmol/h]	Deficit CO_2	$n^-_{CO2} = \begin{cases} (P_{CH4} - P_{CH4,c} - P_{n,oxy})/213 & \text{if } P_{CH4} > P_{CH4,c} + P_{n,oxy} \\ 0 & \text{if } P_{CH4} \le P_{CH4,c} + P_{n,oxy} \end{cases}$
n_{CO2} [kmol/h]	Total CO_2 in the buffer	$n_{CO2\,(j)} = n_{CO2\,(j-1)} + n^+_{CO2\,(j-1)} - n^-_{CO2\,(j-1)}$
W_{ASU} [kW]	Required ASU to fully operate in oxy-fuel	$W_{ASU} = P_{CH4,p}/15.25$

Table 3. Computed variables that depend on cases

Case	H_2 consumption, $P_{H2,c}$ [kW]	Renewable thermal production, Q [kW]	CH_4 directly consumed from PtG, $P_{CH4,c}$ [kW]	CH_4 consumed from network storage, $P_{n,c}$ [kW]
1	P_{100}	Q_d	P_{CH4}	$(Q_d - Q_{100})/\varepsilon_{boil}$
2	P_{100}	$Q_{100} + Q_n$	P_{CH4}	P_n
3	P_{100}	Q_d	P_{CH4}	$(Q_d - Q_{100})/\varepsilon_{boil}$
4	P_{100}	$Q_{100} + Q_n$	P_{CH4}	P_n
5	P_{100}	Q_d	$\begin{cases} (Q - Q_{meth})/\varepsilon_{boil} & \text{if } (Q - Q_{meth}) > 0 \\ 0 & \text{if } (Q - Q_{meth}) \le 0 \end{cases}$	0
6	P_{100}	Q_d	P_{CH4}	$(Q_d - Q_{100})/\varepsilon_{boil}$
7	P_{100}	$Q_{100} + Q_n$	P_{CH4}	P_n
8	$P_{H2} + P_b$	Q_d	P_{CH4}	$(Q_d - Q_{H2} - Q_b)/\varepsilon_{boil}$
9	$P_{H2} + P_b$	$Q_{H2} + Q_b + Q_n$	P_{CH4}	P_n
10	P_{100}	Q_d	$(Q - Q_{meth})/\varepsilon_{boil}$	0
11	$P_{H2} + P_b$	Q_d	$(Q - Q_{meth})/\varepsilon_{boil}$	0
12	$P_{H2} + P_b$	Q_d	P_{CH4}	$(Q_d - Q_{H2} - Q_b)/\varepsilon_{boil}$
13	$P_{H2} + P_b$	$Q_{H2} + Q_b + Q_n$	P_{CH4}	P_n
14	P_{100}	Q_d	$\begin{cases} (Q - Q_{meth})/\varepsilon_{boil} & \text{if } (Q - Q_{meth}) > 0 \\ 0 & \text{if } (Q - Q_{meth}) \le 0 \end{cases}$	0
15	$P_{H2} + P_b$	Q_d	$\begin{cases} (Q - Q_{meth})/\varepsilon_{boil} & \text{if } (Q - Q_{meth}) > 0 \\ 0 & \text{if } (Q - Q_{meth}) \le 0 \end{cases}$	0
16	P_{100}	Q_d	P_{CH4}	$(Q_d - Q_{100})/\varepsilon_{boil}$
17	P_{100}	$Q_{100} + Q_n$	P_{CH4}	P_n
18	$P_{H2} + P_b$	Q_d	P_{CH4}	$(Q_d - Q_{H2} - Q_b)/\varepsilon_{boil}$
19	$P_{H2} + P_b$	$Q_{H2} + Q_b + Q_n$	P_{CH4}	P_n
20	0	Q_d	0	Q_d/ε_{boiler}
21	0	Q_n	0	P_n
22	P_{100}	Q_d	$(Q - Q_{meth})/\varepsilon_{boil}$	0
23	$P_{H2} + P_b$	Q_d	$(Q - Q_{meth})/\varepsilon_{boil}$	0
24	$P_{H2} + P_b$	Q_d	P_{CH4}	$(Q_d - Q_{H2} - Q_b)/\varepsilon_{boil}$
25	$P_{H2} + P_b$	$Q_{H2} + Q_b + Q_n$	P_{CH4}	P_n
26	0	Q_d	0	Q_d/ε_{boil}
27	0	Q_n	0	P_n
28	P_{100}	Q_d	$\begin{cases} (Q - Q_{meth})/\varepsilon_{boil} & \text{if } (Q - Q_{meth}) > 0 \\ 0 & \text{if } (Q - Q_{meth}) \le 0 \end{cases}$	0
29	$P_{H2} + P_b$	Q_d	$\begin{cases} (Q - Q_{meth})/\varepsilon_{boil} & \text{if } (Q - Q_{meth}) > 0 \\ 0 & \text{if } (Q - Q_{meth}) \le 0 \end{cases}$	0
30	0	Q_d	0	Q_d/ε_{boil}
31	0	Q_n	0	P_n
32	P_{100}	Q_d	$\begin{cases} (Q - Q_{meth})/\varepsilon_{boil} & \text{if } (Q - Q_{meth}) > 0 \\ 0 & \text{if } (Q - Q_{meth}) \le 0 \end{cases}$	0
33	$P_{H2} + P_b$	Q_d	$\begin{cases} (Q - Q_{meth})/\varepsilon_{boil} & \text{if } (Q - Q_{meth}) > 0 \\ 0 & \text{if } (Q - Q_{meth}) \le 0 \end{cases}$	0
34	0	Q_d	0	Q_d/ε_{boil}
35	0	Q_n	0	P_n

5. Results and discussion

The analysis of the 9 scenarios set in Table 1 is here presented with the objective of identifying the more suitable situations for the proposed PV-PtG-Oxyfuel system to be implemented. The thermal demand

coverage with PV energy will be calculated, as well as the operating hours of each equipment, the required volume for the H_2, CO_2 and O_2 buffers and the interactions with the natural gas network.

5.1. Solar photovoltaic share, surplus electricity and electrolyzer size

When demand is varied in the studied facility, the share of solar PV in the electricity supply barely changes. Solar production covers demand for a specific period of time during the day, and therefore the amount of directly usable electricity is proportionally reduced when demand decreases. However, the annual coverage is very similar in all cases (Fig. 7). For instance, when the annual electricity demand is 25% greater than solar production, the renewable source covers the 47.0% of annual demand. In the case that demand equals PV production, the solar share is 48.6%. Even when electricity demand is reduced down to represent the 75% of the PV production, the renewable share only reaches the 50.1%.

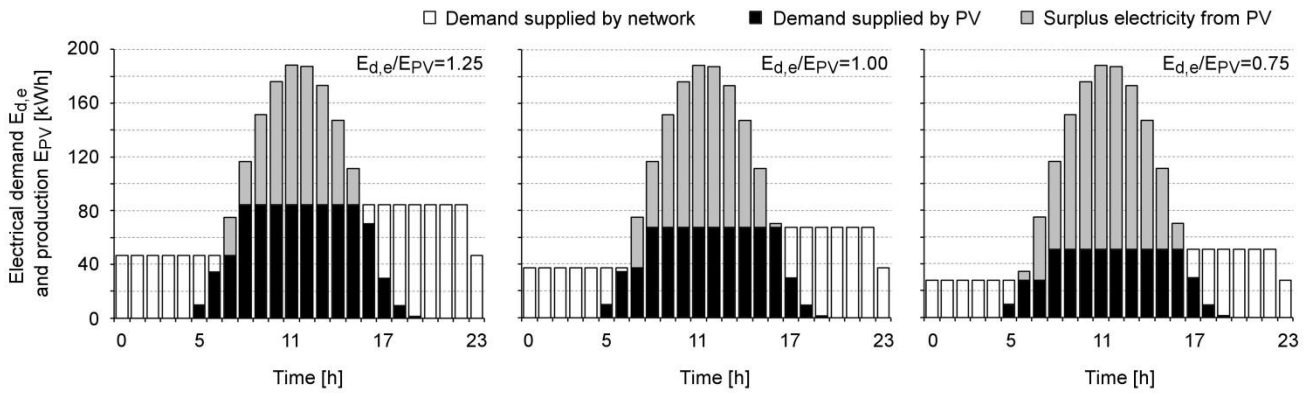

Figure 7. Electrical demand, $E_{d,e}$, and production, E_{PV}, for one typical day of July.

What actually varies with demand is the available surplus electricity. For $E_{d,e}/E_{PV} = 1.25$ the annual excess of solar electricity production is 179.1 MWh, while for $E_{d,e}/E_{PV} = 1.00$ the surplus increases to 222.9 MWh, and for $E_{d,e}/E_{PV} = 0.75$ up to 270.9 MWh. The objective of the following analysis is to compare the coverage of thermal demand with the surplus management in the PtG-Oxyfuel boiler integrated system and the different situations of hydrogen and methane storage, in order to identify which scenarios are more suitable to implement this technology.

The amount of surplus electricity that can be processed will depend on the electrolysis installed capacity. Electrolyzer was sized to maximize the amount of electricity that is stored at nominal load (Fig. 3). Table 4

gathers the optimized electrolysis capacity, $W_{elec,0}$, the energy stored at nominal and partial load and the energy discarded for each ratio $E_{d,e}/E_{PV}$. It is observed that the processed energy at nominal load is above the 50% of the surplus electricity for the three analyzed situations. Besides, the share of dumped energy diminishes for those scenarios of low electric demand with regard PV production, even though the surplus greatly increases. This means that the equivalent operating hours of the electrolyzer system increase from 2184 to 2475 hours. Thus, as for cogeneration systems, two positive effects are shown under relatively low electrical demand: a shorter payback period for the electrolyzer (higher operating hours) and a greater coverage of thermal demand with PV renewable energy

Table 4. Performance of the optimized electrolyzer sizes.

Ratio $E_{d,e}/E_{PV}$	1.25	1.00	0.75
Electrolyzer size, $W_{elec,0}$ [kW]	65	82	96
Surplus electricity from E_{PV} [MWh]	179.1	222.9	270.9
Stored energy at nominal load, $E(h_0)$ [MWh]	92.9	117.2	140.2
Stored energy at partial load, E_{part} [MWh]	49.1	72.7	97.4
Discarded energy, $\boldsymbol{E_{disc}}$ [MWh]	37.1	33.0	33.3
Electrolysis operating hours, h_{elec} [h]	2183.8	2315.2	2475.1

5.2. Management of methanation and buffers: Case distribution

Once the surplus availability is quantified, the methanation system is sized according to the proposed ratios of thermal demand. The results corresponding to the 9 scenarios previously presented are summarized in Table 5. In scenarios 1-5, the maximum hourly thermal demand ($Q_{d,max}$) is above the maximum amount of producible heat (Q_{max}), and therefore there is no limitation in sizing the PtG-Oxyfuel system (see Eq. 9). Accordingly, the operating hours for methanation coincide with those of electrolyzer. It should be noticed that in these cases the air-fired boiler keeps an important role in the heat supply, hence these scenarios are not desirable due to the presence of the two types of boilers.

Conversely, for scenarios 6-9 the producible heat is greater than the maximum thermal demand, so the size of methanation is reduced to avoid oversizing. This leads to a significant increment in the equivalent operating

hours of the methanation system up to 3540 h in scenario 8 and 5311 h in scenario 9, helping the economic amortization of initial inversion.

Table 5. Results of the PV-PtG-Oxyfuel boiler model for the defined scenarios

Scenario	**1**	**2**	**3**	**4**	**5**	**6**	**7**	**8**	**9**
Ratio $E_{d,e}/E_{PV}$	1.25	1.25	1.25	1.00	1.00	1.00	0.75	0.75	0.75
Ratio $E_{d,t}/E_{d,e}$	1.00	0.75	0.50	1.00	0.75	0.50	1.00	0.75	0.50
Electric demand, $E_{d,e}$ [MWh/y]	542.3	542.3	542.3	433.8	433.8	433.8	325.3	325.3	325.3
$E_{d,e}$ covered by E_{PV} [%]	46.7	46.7	46.7	48.6	48.6	48.6	50.0	50.0	50.0
Surplus electricity from E_{PV} [MWh/y]	179.1	179.1	179.1	222.9	222.9	222.9	270.9	270.9	270.9
Electrolyzer size, $W_{elec,0}$ [kW]	65.0	65.0	65.0	82.0	82.0	82.0	96.0	96.0	96.0
Electrolysis operating hours, h_{elec} [h]	2183.8	2183.8	2183.8	2315.2	2315.2	2315.2	2475.1	2475.1	2475.1
Stored surplus electricity [%]	79.3	79.3	79.3	85.2	85.2	85.2	87.7	87.7	87.7
Methanation size (H_2 input), $P_{meth,0}$ [kW]	45.5	45.5	45.5	57.4	57.4	41.8	62.6	47.0	31.3
Methanation operating hours [h]	2183.8	2183.8	2183.8	2315.0	2315.0	3182.3	2655.5	3540.7	5311.1
Exothermal heat [MWh/y]	15.6	15.6	15.6	20.8	20.8	20.8	26.1	26.1	26.1
Produced SNG [MWh/y]	80.6	80.6	80.6	107.8	107.8	107.8	134.9	134.9	134.9
SNG directly consumed [%]	100.0	98.5	84.4	96.2	82.3	71.6	74.7	71.7	69.1
SNG stored in the network [%]	0.0	1.5	15.6	3.8	17.7	28.4	25.3	28.3	30.9
SNG recovered from network [%]	-	100.0	100.0	100.0	100.0	100.0	100.0	100.0	100.0
to the oxy-fuel boiler	-	100.0	99.6	100.0	100.0	100.0	100.0	100.0	100.0
to the air-fired boiler	-	0.0	0.4	0.0	0.0	0.0	0.0	0.0	0.0
Oxy-boiler size (CH_4 input), $P_{boil,0}$ [kW]	36.9	36.9	36.9	46.5	46.5	41.6	62.3	46.8	31.2
Thermal demand, $E_{d,t}$ [MWh/y]	542.3	406.7	271.1	433.8	325.3	216.9	325.3	244.0	162.7
$E_{d,t}$ covered by PtG [%]	15.5	20.7	31.0	25.9	34.6	51.8	43.3	57.7	86.5
H_2 buffer size [m^3 (NTP)]	6.0	6.0	6.0	7.3	7.3	32.2	9.2	43.9	89.2
O_2 buffer size [m^3 (NTP)]	3.0	8.2	36.5	19.6	36.8	101.4	57.6	376.0	3676.6
CO_2 buffer size [m^3 (NTP)]	-	4.2	18.6	10.0	18.7	48.6	28.5	188.1	1861.3
Required NG to complete demand [MWh/y]	539.1	379.6	220.1	378.1	250.5	122.9	217.2	121.5	25.8
Required ASU to run only in oxy-fuel [kW]	6.8	5.1	3.4	5.4	4.1	2.7	4.1	3.1	2.0
ASU consumption to run only in oxy-fuel [MWh/y]	35.3	24.9	14.4	24.8	16.4	8.1	14.2	8.0	1.7

The proper sizing of the PtG-Oxyfuel boiler equipment has a direct influence on the case distribution of Fig. 4 and 5, which will define the management of the system. When the size of the buffers is not limited (i.e., there is no vent of O_2 or CO_2 to the atmosphere), the case distribution is the one depicted in Fig. 8 (cases with less than 1% share are not presented). In general, cases 21 and 27 are the most common situations since they appear in every proposed scenario. These two cases take place when solar production is not enough to operate the methanation plant (even using the H_2 from the buffer) at the same time that the synthetic natural gas previously stored in the network is insufficient to satisfy thermal demand. In practice, these situations correspond to nighttime periods and scenarios with a characteristic short-term storage of the introduced SNG

in the network. The latter effect can be identified by comparing scenarios 8 and 9, in which the stored amount of SNG is similar but only in scenario 9 it is predominantly recovered without depleting the stored methane (23.4% of presence for case 26). Hence, scenario 9 is actually favoring the utilization of long-term storage technologies like PtG.

Regarding the periods in which SNG is stored in the network, the most common situation is case 5, with 28.5% share in scenario 9 and progressively decreasing down to 2.1% for scenario 2 (scenario 1 has no injection of SNG to the network). Besides, scenario 9 has a remarkable contribution of case 22 to the process of storing surplus in the gas grid, which is mainly conducted with hydrogen from the buffer.

The size of the O_2 and CO_2 buffers greatly increases as the time of the SNG storage increases, so high-pressurized buffers must be considered for some scenarios. Nevertheless, the management of the produced hydrogen and its conversion to methane for its injection in the gas grid allows keeping the size of H_2 buffer below 90 m^3(NTP) for all scenarios. Potential solutions for the reduction of the O_2 and CO_2 buffers could be operating an air separation unit or directly injecting part of the H_2 in the gas network, respectively. Both possibilities should be economically assessed for each specific situation.

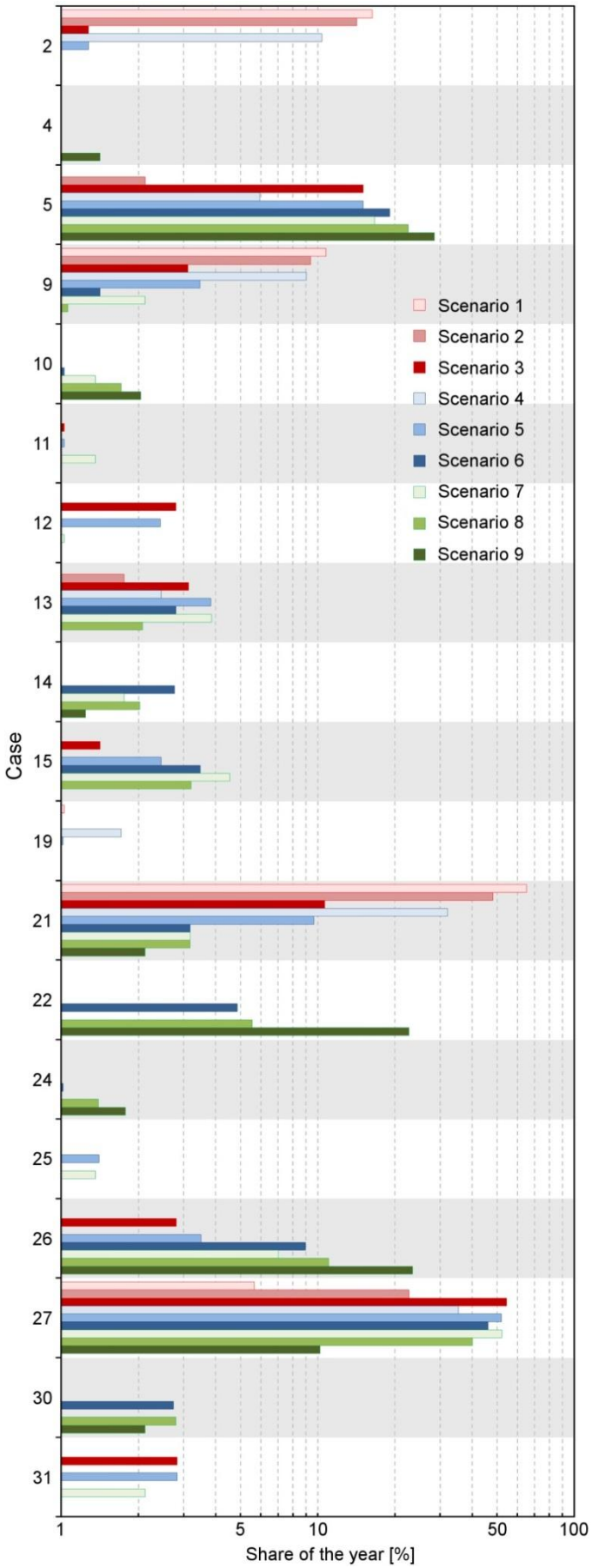

Figure 8. Distribution of case presence in a year for scenarios 1-9.

5.3. SNG share in thermal demand and temporary displacement of surplus

Under the proposed scenarios, the percentage of thermal demand that can be covered with SNG ranges between 15.5% and 86.5%. However, as thermal demand always exists at the same time than surplus electricity, part of the generated SNG is consumed as soon as it is produced, and therefore the temporary displacement is limited. Only when SNG is also an excess, the PtG system injects methane into the gas network and the integrated facility takes advantage regarding conventional storage technologies with short-time energy reuse.

The percentage of synthetic methane stored in the gas grid varies from 0.0% in scenario 1 (no injection required) to 30.9% in scenario 9. Nevertheless, most scenarios recover the SNG from the network within a few hours of its previous injection, because either surplus SNG is low or thermal demand is high. This behavior can be seen in Fig. 9 for scenario 7, where the periodic peaks of stored SNG alternate with the emptying of the storage (scenarios 1-5 present the same behavior than scenario 7, but proportionally reduced according to the amount of injected SNG). Only in scenarios 6, 8 and 9 a temporary displacement beyond the month exists. Scenarios 6 and 8 store SNG during august to be rapidly consumed at the beginning of September. Meanwhile, the lower thermal demand of scenario 9 allows storing surplus SNG since April to be used 6 months later, throughout October, November and December.

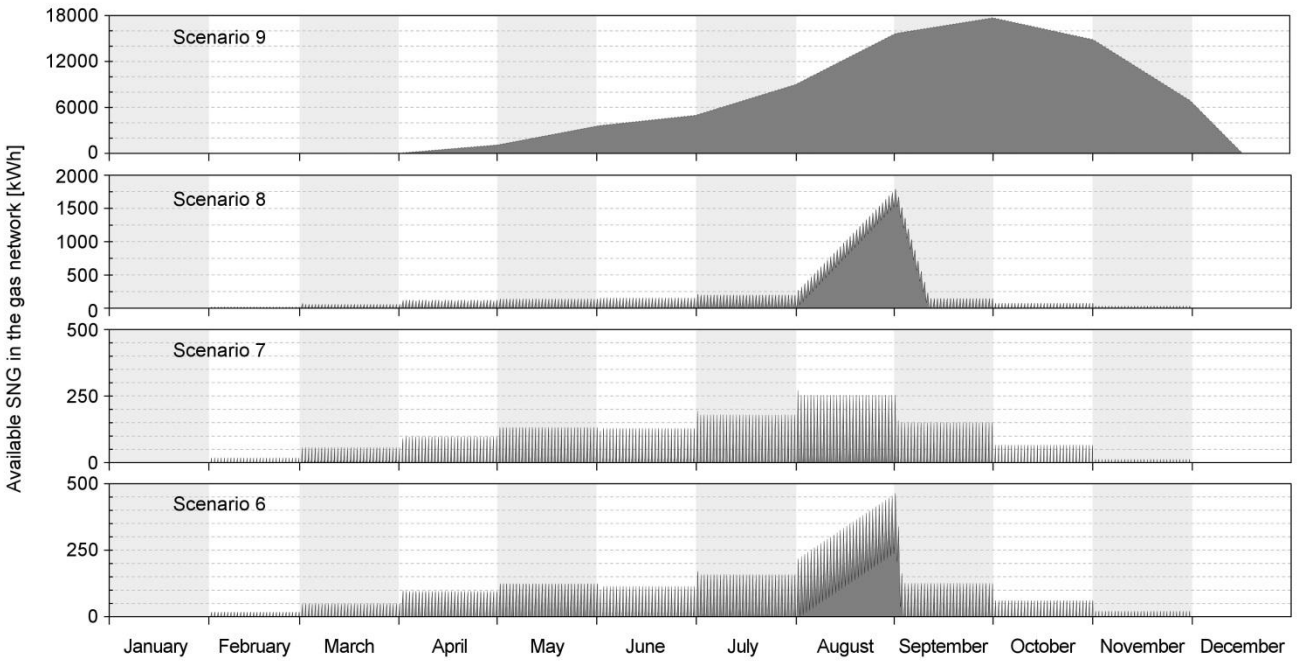

Figure 9. Available SNG in the gas network for scenarios 6-9.

Hence, the utilization of the PtG-Oxyfuel boiler system in scenarios 1-5 and 7 should be discouraged since there are better options with greater efficiencies to store surplus electricity in hourly periods. For example, the Li-ion batteries are commercially available up to 100 kW, with storage durations from hours to several days, and efficiencies between 85% and 90%. Besides, the capital cost of this technology (1200 – 4000 $/kW) is much lower than that of Power to Gas (10000 $/kW) [28]. However, this kind of solution by itself would not decarbonize the thermal supply of the building. Thus, in addition to batteries, the utilization of hybrid photovoltaic thermal solar collectors (production of electricity and heat in the same panel) coupled with thermal storage (hot water tanks) could solve this issue [29]. The appropriate size of such system would have to be studied to meet the electrical and thermal demands of the building.

Only in scenarios 6, 8 and 9, the long-term energy storage is necessary. It has to be said that, besides the technical analysis, a specific economic evaluation may be assessed to clarify in scenarios 6, 8 and 9 the adequacy of combining PtG with short-term storage technologies, like batteries and hybrid solar panels, for the first quarter of the year.

Due to the novelty of the concept (combination of PV, Power to Gas and Oxy-fuel combustion) and application (Power to Gas as long-term energy storage for zero-emission buildings), there is a lack of comparable studies in literature to discuss results with previous findings. The closest studies are those of Santoli et al. [30], which analyzed the application of hybrid photovoltaic thermal solar collectors for Power to Hydrogen systems in buildings, concluding that its combination with gas heat pumps seems to be competitive. In general, energy storage devices are highly recommended for PV generation in buildings, since the utilization of the renewable production may increase from the 35% to the 77% [31]. In our study, the utilization of solar production increases from 37.5% to 92.3% when long-term storage becomes advantageous, i.e., in scenario 9.

6. Conclusions

A cogeneration system for urban buildings has been proposed and analyzed, comprising solar photovoltaic, Power to Gas, and an oxy-fuel boiler. Solar photovoltaic supplies electricity demand and provides, whenever

exists, excess electricity to the Power to Gas system to produce methane. The oxy-fuel boiler partially covers thermal demand with this synthetic natural gas. The integration of the byproduct oxygen from electrolysis, into the oxy-fuel boiler, allows gathering the CO_2 for methanation without energy penalty.

A methodology has been developed for the design, sizing and operation of energy storage installations based on Power to Gas, and for the design of control strategies that facilitate a positive economic balance. The decision-making tree of the whole potential situations that might occur while operating the PV-PtG-Oxyfuel system has been presented. The mathematical description allows performing a continuous characterization of the energy and mass flows of the system throughout the year, as well as sizing the intermediate buffers required.

In the present study, the application of PV-PtG-Oxyfuel systems to cover the energy demand of a typical sports center in Zaragoza (Spain) is assessed, and the most suitable scenarios for its implementation are established. The selected location is characterized by a 270 kW installed photovoltaic capacity and an annual renewable production of 433.8 MWh. A total of 9 potential energy scenarios are proposed, for which solar production covers the 46.7% – 50.0% of the electricity demand. The optimized capacities of electrolysis to gather the excess electricity vary between 65 kW and 96 kW, with operating hours in the range 2184 - 2475 hours. The percentage of dumped surplus electricity is always below the 21% of the total surplus (i.e., below the 9% of total solar photovoltaic production).

The annual production of synthetic natural gas under this framework amounts to 80.6 – 134.9 MWh. The percentage of thermal demand that can be covered with this synthetic methane widely varies between 15.5% and 86.5% depending on the scenario. Besides, the percentage of methane that is stored in the gas grid varies from 0.0% (no injection required) to 30.9%. However, not every scenario makes the most of Power to Gas technology in terms of energy storage. Most scenarios recover the methane from the network within a few hours of its previous injection (scenarios 1 - 5 and 7). The utilization of the PtG-Oxyfuel boiler system in these scenarios should be discouraged since there are better options with greater efficiencies to store surplus electricity in hourly periods. Only in scenarios 6, 8 and 9, the long-term energy storage of Power to Gas technology is necessary. Scenarios 6 and 8 store synthetic natural gas during august to be rapidly consumed at

the beginning of September. Meanwhile, scenario 9 stores surplus synthetic methane since April to October, to be used throughout the last quarter of the year.

This behavior can be understood in detail when observing the case distribution. The most common situations are cases 21 and 27, corresponding to nighttime periods and scenarios with a characteristic short-term storage of the introduced synthetic gas in the network. Only in scenario 9 the synthetic methane is predominantly recovered without depleting the stored resource (23.4% of presence for case 26). Regarding the periods in which synthetic natural gas is stored in the network, the most common situation is case 5 (i.e., low thermal demand and methanation operating at full load), with 28.5% share in scenario 9 and progressively decreasing down to 2.1% for scenario 2 (scenario 1 has no injection of synthetic natural gas to the network). Besides, scenario 9 has a remarkable contribution of case 22 to the process of storing surplus in the gas grid, which is mainly conducted with hydrogen from the buffer.

From these results, economic evaluations may be assessed to clarify the adequacy of combining PtG with solar photovoltaic systems in urban buildings. The proposed methodology is a first approach to the development of a full algorithm of control and scheduling. In the present work, the limitations and the possible operating situations are established to serve as technical base of future control algorithms. Economic variables must be considered in such case, to take into account fixed and variable costs, purchase and sale prices of the involved gases and incomes for the avoided CO_2 emissions. Therefore, it will serve as basis of advanced control algorithms to reach a positive economic balance.

Acknowledgements

The work described in this paper is supported by the R+D Spanish National Program from Ministerio de Economía y Competitividad, MINECO (Spanish Ministry of Economy and Competitiveness) and the European Regional Development Funds (European Commission), under project ENE2016-76850-R. Financial support for M.B. during his Ph.D. studies was co-funded by the Department of Industry and Innovation of Diputación General de Aragón, and by the European Social Fund.

Appendix – Oxygen deficit and surplus criterion

The actual criterion to discern when there is a deficit or a surplus of oxygen is actually given by Eq. (A.1), since the PtG-Oxyfuel system is designed to close the O_2 balance (i.e., the by-product O_2 that is generated when producing hydrogen at rate P_{H2} matches the required O_2 in the boiler when the consumed methane is $P_{CH4,c} = P_{H2} \cdot \eta_{CH4}$). The Eq. A.1 compares the amount of hydrogen produced with the quantity that should be produced to close the O_2 balance, according to the amount of methane that is introduced into the oxy-fuel boiler. The > symbol implies a surplus, and the < symbol a deficit.

$$\mathrm{P_{H2}} \lessgtr \frac{\mathrm{P_{CH4,c}+P_{n,oxy}}}{\mathrm{\eta_{CH4}}} \tag{A.1}$$

To relate this expression with the heat demand (Q_d) and the heat produced from hydrogen (Q_{H2}), the following steps must be considered (Eq. A.2 – Eq. A.8):

$$\mathrm{P_{H2} \cdot \eta_{CH4} \lessgtr P_{CH4,c} + P_{n,oxy}} \tag{A.2}$$

$$\mathrm{P_{H2} \cdot \eta_{CH4} \cdot \varepsilon_{boil} + P_{H2} \cdot \varepsilon_{meth} \lessgtr \left(P_{CH4,c} + P_{n,oxy}\right) \cdot \varepsilon_{boil} + P_{H2} \cdot \varepsilon_{meth}} \tag{A.3}$$

$$\mathrm{Q_{H2} \lessgtr \left(P_{CH4,c} + P_{n,oxy}\right) \cdot \varepsilon_{boil} + P_{H2,c} \cdot \varepsilon_{meth} - P_{H2,c} \cdot \varepsilon_{meth} + P_{H2} \cdot \varepsilon_{meth}} \tag{A.4}$$

$$\mathrm{Q_{H2} \lessgtr Q + (P_{H2} - P_{H2,c}) \cdot \varepsilon_{meth}} \tag{A.5}$$

Where Q is the renewable thermal production, which reaches thermal demand (Q_d) in cases 1 and 3. Thus, for the respective situation:

$$\mathrm{Q_{H2} \lessgtr Q_d + (P_{H2} - P_{H2,c}) \cdot \varepsilon_{meth}} \tag{A.6}$$

$$\mathrm{Q_{H2} - (P_{H2} - P_{H2,c}) \cdot \varepsilon_{meth} \lessgtr Q_d} \tag{A.7}$$

Since in general $\mathrm{Q_{H2} \gg (P_{H2} - P_{H2,c}) \cdot \varepsilon_{meth}}$, the last condition can be approximated to:

$$\mathrm{Q_{H2} \lessgtr Q_d} \tag{A.8}$$

Where, $Q_{H2} > Q_d$ implies a surplus of O_2, and $Q_{H2} < Q_d$ a deficit. For this reason, the relative comparison between Q_{H2} and Q_d is included in the second step of the tree decision of Figure 4, in order to potentially

differentiate those situations that are only distinguishable through the surplus and deficit of O_2 (e.g., cases 1 and 3).

Nomenclature

Variable

A	[m^2]	Area
E	[kWh]	Energy
h	[h]	Hours of operation
n	[kmol/h]	Mol flow
P	[kW]	Power related to the energy contained in a flow of a chemical product
Q	[kW]	Thermal power
W	[kW]	Electric power
ε	[-]	Efficiency towards thermal energy production
η	[-]	Efficiency towards the production of electricity or a chemical product

Subscript

0	Nominal operation / Optimal point
100	Full operation load
40	Minimum operation load
ASU	Air separation unit
b	Buffer of hydrogen
boil	Boiler
c	Related to a quantity that is consumed
CH_4	Methane / Methanation process
CO_2	Carbon dioxide
d	Related to a quantity that is demanded
disc	Related to a quantity that is discarded
e	Electric energy
elec	Electrolyzer
H_2	Hydrogen / Electrolysis process
j	Index to specify hour j
max	Maximum value
meth	Methanation
n	Gas network
p	Related to a quantity that is purchased
part	Partial load
PV	Solar photovoltaic panels
roof	Roof of the building
s	Surplus
t	Thermal energy
year	Accounting an annual period

Superscript

+	Surplus
-	Deficit

References

[1] European Parliament. Directive 2009/28/EC of the European Parliament and of the Council of 23 April 2009. 2009.

[2] Capros P, Vita A De, Tasios N, Siskos P, Kannavou M, Petropoulos A, et al. EU Reference Scenario 2016: Energy, transport and GHG emissions. Trends to 2050. European Union; 2016. doi:10.2833/9127.

[3] Vandewalle J, Bruninx K, D'haeseleer W. Effects of large-scale power to gas conversion on the power, gas and carbon sectors and their interactions. Energy Convers Manag 2015;94:28–39. doi:10.1016/j.enconman.2015.01.038.

[4] Bailera M, Kezibri N, Romeo LM, Espatolero S, Lisbona P, Bouallou C. Future applications of hydrogen production and CO2 utilization for energy storage: Hybrid Power to Gas-Oxycombustion power plants. Int J Hydrogen Energy 2017;42. doi:10.1016/j.ijhydene.2017.02.123.

[5] Bailera M, Espatolero S, Lisbona P, Romeo LM. Power to gas-electrochemical industry hybrid systems: A case study. Appl Energy 2017;202. doi:10.1016/j.apenergy.2017.05.177.

[6] Bailera M, Lisbona P, Romeo LM, Espatolero S. Power to Gas-biomass oxycombustion hybrid system: Energy integration and potential applications. Appl Energy 2016;167. doi:10.1016/j.apenergy.2015.10.014.

[7] Llera E, Romeo LM, Bailera M, Osorio JL. Exploring the integration of the power to gas technologies and the sustainable transport. Int J Energy Prod Manag 2018;3:1–9. doi:10.2495/EQ-V3-N1-1-9.

[8] Bailera M, Lisbona P, Romeo LM, Espatolero S. Power to Gas projects review: Lab, pilot and demo plants for storing renewable energy and CO2. Renew Sustain Energy Rev 2017;69:292–312. doi:10.1016/j.rser.2016.11.130.

[9] Bailera M, Lisbona P, Romeo LM. Power to gas-oxyfuel boiler hybrid systems. Int J Hydrogen Energy 2015;40:10168–75. doi:10.1016/j.ijhydene.2015.06.074.

[10] Gao J, Wang Y, Ping Y, Hu D, Xu G, Gu F, et al. A thermodynamic analysis of methanation reactions of carbon oxides for the production of synthetic natural gas. RSC Adv 2012;2:2358. doi:10.1039/c2ra00632d.

[11] Abanades JC, Rubin ES, Mazzotti M, Herzog HJ. On the climate change mitigation potential of CO_2 conversion to fuels. Energy Environ Sci 2017;10:2491–9. doi:10.1039/C7EE02819A.

[12] He L, Lu Z, Zhang J, Geng L, Zhao H, Li X. Low-carbon economic dispatch for electricity and natural gas systems considering carbon capture systems and power-to-gas. Appl Energy 2018;224:357–70. doi:10.1016/j.apenergy.2018.04.119.

[13] Li G, Zhang R, Jiang T, Chen H, Bai L, Li X. Security-constrained bi-level economic dispatch model for integrated natural gas and electricity systems considering wind power and power-to-gas process. Appl Energy 2017;194:696–704. doi:10.1016/j.apenergy.2016.07.077.

[14] McKenna RC, Bchini Q, Weinand JM, Michaelis J, König S, Köppel W, et al. The future role of Power-to-Gas in the energy transition: Regional and local techno-economic analyses in Baden-Württemberg. Appl Energy 2018;212:386–400. doi:10.1016/j.apenergy.2017.12.017.

[15] Wilson IAG, Styring P. Why Synthetic Fuels Are Necessary in Future Energy Systems. Front Energy Res 2017;5:1–10. doi:10.3389/fenrg.2017.00019.

[16] Kotowicz J, Węcel D, Jurczyk M. Analysis of component operation in power-to-gas-to-power installations. Appl Energy 2018;216:45–59. doi:10.1016/j.apenergy.2018.02.050.

[17] Abedi S, Alimardani A, Gharehpetian GB, Riahy GH, Hosseinian SH. A comprehensive method for optimal power management and design of hybrid RES-based autonomous energy systems. Renew Sustain Energy Rev 2012;16:1577–87. doi:10.1016/j.rser.2011.11.030.

[18] Sun G, Chen S, Wei Z, Chen S. Multi-period integrated natural gas and electric power system probabilistic optimal power flow incorporating power-to-gas units. J Mod Power Syst Clean Energy 2017;5:412–23. doi:10.1007/s40565-017-0276-1.

[19] Ye J, Yuan R. Integrated Natural Gas, Heat, and Power Dispatch Considering Wind Power and Power-to-Gas. Sustainability 2017;9:602. doi:10.3390/su9040602.

[20] Parra D, Zhang X, Bauer C, Patel MK. An integrated techno-economic and life cycle environmental assessment of power-to-gas systems. Appl Energy 2017;193:440–54. doi:10.1016/j.apenergy.2017.02.063.

[21] Parra D, Patel MK. Techno-economic implications of the electrolyser technology and size for power-to-gas systems. Int J Hydrogen Energy 2016;41:3748–61. doi:10.1016/j.ijhydene.2015.12.160.

[22] Guilera J, Ramon Morante J, Andreu T. Economic viability of SNG production from power and CO2. Energy Convers Manag 2018;162:218–24. doi:10.1016/j.enconman.2018.02.037.

[23] Götz M, Lefebvre J, Mörs F, McDaniel Koch A, Graf F, Bajohr S, et al. Renewable Power-to-Gas: A technological and economic review. Renew Energy 2016;85:1371–90.

[24] Koponen J, Kosonen A, Huoman K, Ahola J, Ahonen T, Ruuskanen V. Specific Energy Consumption of PEM Water Electrolysers in Atmospheric and Pressurised Conditions. Proc. 18th Eur. Conf. Power Electron. Appl., 2016.

[25] European Commission. PVGIS - Photovoltaic geographical information system 2018. http://re.jrc.ec.europa.eu/pvg_tools/en/tools.html#PVP (accessed January 31, 2018).

[26] Píriz AG. Auditoría energética en una piscina climatizada (Master's Thesis). 2009.

[27] Ducar IA. Study on Energy Efficiency and Energy Saving Potential in San Agustin Sports Centre. 2017.

[28] Bailera M. Renewable methane. Integrated configurations of power-to-gas and carbon capture by means of renewable energy surplus (Doctoral Thesis). University of Zaragoza, 2017.

[29] Yang DJ, Yuan ZF, Lee PH, Yin HM. Simulation and experimental validation of heat transfer in a novel hybrid solar panel. Int J Heat Mass Transf 2012;55:1076–82. doi:10.1016/j.ijheatmasstransfer.2011.10.003.

[30] de Santoli L, Lo Basso G, Nastasi B. The Potential of Hydrogen Enriched Natural Gas deriving from Power-to-Gas option in Building Energy Retrofitting. Energy Build 2017;149:424–36. doi:10.1016/j.enbuild.2017.05.049.

[31] Del Pero C, Aste N, Paksoy H, Haghighat F, Grillo S, Leonforte F. Energy storage key performance indicators for building application. Sustain Cities Soc 2018;40:54–65. doi:10.1016/j.scs.2018.01.052.